

Thermal Conductivity of High Strength Polyethylene Fiber in Low Temperature

ATSUHIKO YAMANAKA,¹ HIROYUKI FUJISHIRO,² TOSHIHIRO KASHIMA,³ TOORU KITAGAWA,⁴ KIMIKO EMA,⁵ YOSHINOBU IZUMI,⁵ MANABU IKEBE,² SHIGEHIRO NISHIJIMA⁵

¹Advanced Textile R & D Center, Research Center, Toyobo Co., Ltd., 2-1-1, Katata, Ohtsu, Shiga 520-0292, Japan

²Department of Materials Science and Technology, Faculty of Engineering, Iwate University, Ueda 4-3-5, Morioka 020-8551, Japan

³Hamamatsu Technopolis, Shizuoka University, Hamamatsu, Shizuoka 431-3215, Japan

⁴Polymer Institute, Toyobo Research Center Co., Ltd., 2-1-1, Katata, Ohtsu, Shiga 520-0292, Japan

⁵Department of Nuclear Engineering, Graduate School of Engineering, Osaka University, Yamadaoka 2-1, Suita, Osaka 565-0871, Japan

Received 26 November 2004; revised 25 January 2005; accepted 26 January 2005

DOI: 10.1002/polb.20428

Published online in Wiley InterScience (www.interscience.wiley.com).

ABSTRACT: High strength polyethylene fiber (Toyobo, Dyneema[®] fiber, hereinafter abbreviated to DF) used as reinforcement of fiber-reinforced plastics for cryogenic use has a high thermal conductivity. To understand the thermal conductivity of DF, the relation between fiber structure and thermal conductivity of several kinds of polyethylene fibers having different modulus from 15 to 134 GPa (hereinafter abbreviated to DFs) was investigated. The mechanical series-parallel model composed of crystal and amorphous was applied to DFs for thermal conductivity. This mechanical model was obtained by crystallinity and crystal orientation angle measured by solid state NMR and X-ray. Thermal conductivity of DF in fiber direction was dominated by that of the continuous crystal region. The thermal conductivity of the continuous crystal part estimated by the mechanical model increases from 16 to 900 mw/cmK by the increasing temperature from 10 to 150K, and thermal diffusivity of the continuous crystal part was estimated to about 100 mm²/s, which is almost temperature independent. The phonon mean free path of the continuous crystal region of DF obtained by thermal diffusivity is almost temperature independent and its value about 200 Å. With the aforementioned, the mechanical series-parallel model composed of crystal and amorphous regions could be applied to DFs for thermal conductivity. ©2005 Wiley Periodicals, Inc. *J Polym Sci Part B: Polym Phys* 43: 1495–1503, 2005

Keywords: thermal conductivity; polyethylene fiber; low temperature

INTRODUCTION

The thermal conductivity of amorphous polymers is believed to be lower than that of metals or

semiconductors.^{1,2} Therefore, polymers are frequently used as heat insulators. However, in the case of polyethylene crystals, reports have been produced suggesting that crystalline polymers possess high-thermal conductivity toward the direction of the molecular chain axis.^{3–9} The thermal conductivity of electrical insulators can be due to phonons.^{3,5} Therefore, the thermal conduc-

Correspondence to: A. Yamanaka (E-mail: atsuhiko_yamanaka@kt.toyobo.co.jp)

Journal of Polymer Science: Part B: Polymer Physics, Vol. 43, 1495–1503 (2005)
©2005 Wiley Periodicals, Inc.

tivity of crystalline polymer materials depends on their crystallinity and orientation, that is, highly-crystalline and highly-oriented polymers should exhibit high thermal conductivity.⁴⁻⁹ Furthermore, there are high-crystallinity and high-strength fibers that possess thermal conductivity almost as high as metals; these include high-strength polyethylene^{5,10,11} and high-strength polybenzobisoxazole fibers.¹⁰ Thermal conductivity of crystal polymer, for example, polyethylene, was analyzed by a mechanical model composed of crystal and amorphous.^{4,7-9,12-14}

Meanwhile, the importance of polymer materials as electrical insulating or structural materials has been recognized in those areas of cryogenic engineering that require superconducting technology, such as superconducting power equipment, magnetic levitated transportation, medical diagnosis equipment, or nuclear fusion reactors and so on. To apply polymer materials to these areas, their thermal properties, and in particular their coefficient of linear expansion and their thermal conductivity, have been important parameters to study. For example, high-strength polyethylene fiber (Toyobo, Dyneema[®]; DF)¹⁵⁻¹⁷ and composite materials that use DF as a reinforcing fiber (DFRP),^{16,18} possess a negative coefficient of linear expansion toward the direction of the fiber axis. Typical applications for these materials are as coil bobbins¹⁹⁻²⁹ and spacers^{23,28,30,31} for superconductors.

Furthermore, in the field of high-temperature superconducting coils, highly thermal conductive and electrical insulating materials need to be developed to protect superconducting materials from heat burn up.^{32,33} Because DFRP-based materials possess high-thermal conductivity¹⁰ and are highly insulating,³⁴ their application to this system has been expected. Practical reports have been produced concerning the heat-radiation effects of high-temperature superconducting tape materials.^{32,33} These indicate that the thermal conductivity of these insulators as well as their negative expansivity are important characteristics when considering their application in the field of cryogenics.

In this article, we investigate the relationship between the thermal conductivity and the structure of polyethylene fibers (hereafter DFs) having different tensile modulus (from 15 to 134 GPa) to understand the thermal conductivity of DF, which is used as reinforcing fiber in the cryogenic composite material DFRP. Previous reports showed that these DFs exhibited higher

thermal conductivity with increasing tensile modulus.¹¹ Furthermore, a previous report elucidated that DF with higher tensile modulus showed higher negative thermal expansivity, and this relationship was explained by the fiber structure illustrated in the mechanical serial-parallel model (Takayanagi-model), which consists of a crystalline/amorphous structure.¹⁷ In this article, we apply this mechanical model introduced in our previous report¹⁷ to the DFs for thermal conductivity. This mechanical model is composed of the following two parts by parallel combination. One of them is the continuous crystal part, and the other is the series combination part of crystal and amorphous. We estimate the thermal conductivity and thermal diffusivity of the continuous crystal part in DF on the mechanical model.

EXPERIMENTAL

Sample

Four kinds of DFs (Toyobo, Dyneema[®], DF (A-D) with different draw ratio¹⁶ were used.¹⁷ They have different modulus¹⁷ shown as follows: DF(A): 15GPa, DF(B): 51GPa, DF(C): 85GPa, and DF(D): 134GPa.

Measurements

Thermal Conductivity

Thermal conductivity (κ) was measured by a steady-state heat flow method.¹⁰ The measurements of κ were carried out on the automated measuring system with thermal controller of a Gifford-MacMahon (GM) cycle helium refrigerator as a cryostat.³⁵ The fiber samples were prepared by bundling about 6000 monofilaments with a length of 45 mm.^{10,11} The diameters of DFs were about 12 ~ 25 μm . The direction of measurements of κ was parallel to the fiber direction. Details of the determination of κ are described elsewhere.^{10,11}

Crystallinity

Crystallinities of DFs were estimated by peak separation of solid state high resolution NMR. Solid state NMR measurements were carried out on a Varian XL-300 (¹³C, 75.5MHz). NMR spectra were measured by the Cross-Polarization (CP) high power proton dipole decoupling (DD) magic

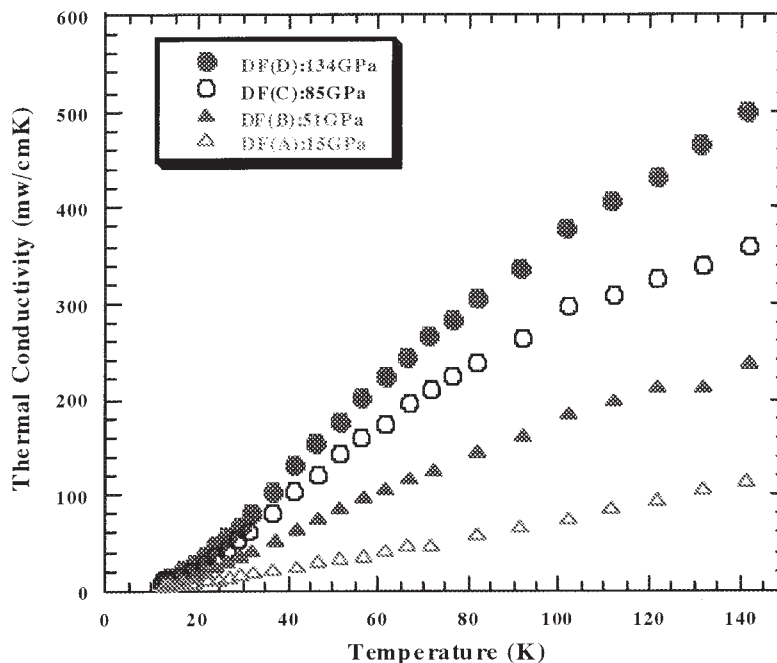


Figure 1. The temperature dependence of thermal conductivity of DF(A–D) in the fiber direction.

angle spinning (MAS) method. Pulse width was 5 ms, dipole DD power was 50 kHz, and MAS rate was 3.5 kHz. Details of NMR measurements were described in a previous article.¹⁷

Orientation Angle

Orientation angle of crystalline phase in DFs was estimated by intensity distribution of X-ray diffraction spots as described in a previous article.¹⁷ A Rigaku RU-200 (40 kV \times 100 mA) was used with X-ray diffraction on Ni-filtered Cu K α ($\lambda = 0.1548$ nm).

RESULTS AND DISCUSSION

Thermal Conductivity of DFs

The temperature dependence of thermal conductivity of DFs in the fiber direction is shown in Figure 1. Thermal conductivity increases with increasing tensile modulus of DF, and all of them increase with increasing temperature. It is known that thermal conduction of polyethylene is caused by phonon conduction and that thermal conductivity is higher in the chain axis combined by covalent bonding than perpendicular to the chain axis combined by van der Waals interaction in the crystal region.^{3,7,14} It is also known that thermal con-

ductivity in the amorphous region is much lower than that in the crystal region in the chain axis.⁸ From these results, the relation between the thermal conductivity and tensile modulus of DFs in the fiber direction is inferred to be caused by the crystallinity and orientation angles.

The crystallinities and orientation angles of DFs are measured by solid state high resolution NMR and X-ray diffraction in the following sections. From those results, the parameters of the mechanical series-parallel model are estimated to explain the thermal conductivity of DFs.

Crystallinity of DFs

It is known that the crystal and amorphous of polyethylene have different chemical shifts in solid state ^{13}C NMR spectra.^{36–40} This means that it is possible to estimate the crystallinity by peak separation of the ^{13}C NMR spectra of polyethylene.^{36–40} In this way, the crystallinities of DFs were estimated by the measurements of solid state ^{13}C NMR spectra in a previous work.¹⁷ The details of estimation of crystallinities were discussed in a previous article.¹⁷ The crystallinities of DFs are shown in Figure 2. It is shown that crystallinity is higher in DFs of higher modulus. Relations between the thermal conductivities at 20, 50, 80, and 100K and crystallinities of DFs are shown in

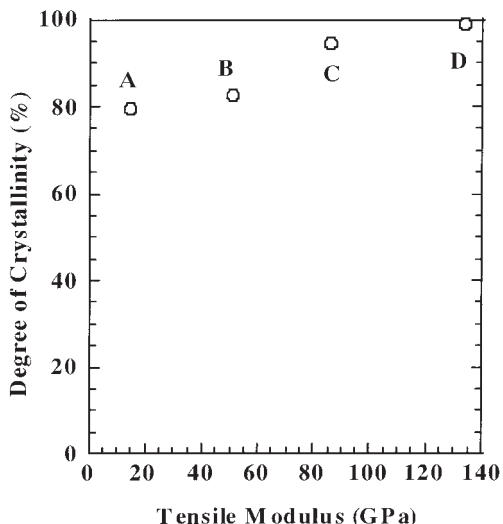


Figure 2. Crystallinity and tensile modulus of DF(A–D).

Figure 3. It is shown that thermal conductivity of DF increases with increasing crystallinity. This suggests a contribution of the crystal region to the high thermal conductivity of DF. But thermal conductivities between DF(A) and DF(B) are much different in spite of a small difference of crystallinities. Therefore, the increasing thermal conductivity cannot be explained only by crystallinities of DFs. In the following section, orientation angles of DFs are reported.

Orientation Angles of DFs

The orientation angles of DFs are shown in Figure 4.¹⁷ The orientation angle is smaller;

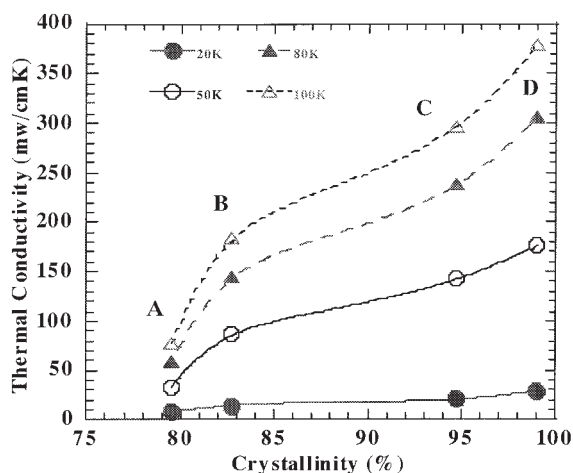


Figure 3. Relation of crystallinities and thermal conductivities at 20, 50, 80, and 100K of DFs.

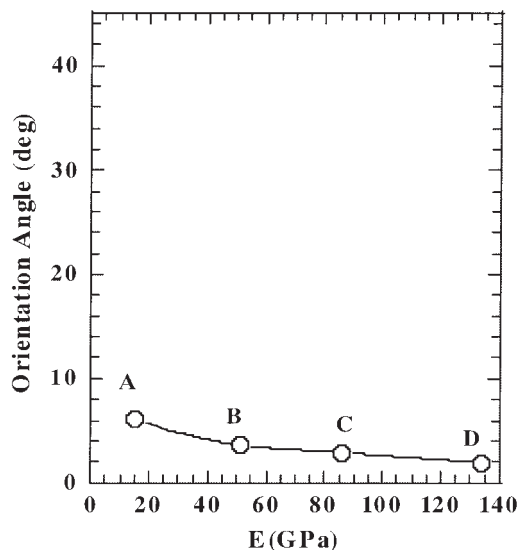


Figure 4. Orientation angles and tensile modulus of DF(A–D).

the tensile modulus is higher. Relations between the thermal conductivities at 20,50,80, and 100K and orientation angles of DFs are shown in Figure 5. Therefore we found that highly oriented DF has a high thermal conductivity.

But every DF has a small orientation angle from 1.9deg to 6.1deg, which is nearly equal to 0. In this section, the contribution of the orientation angle to the thermal conductivity of the DFs is estimated. Thermal conductivity of the crystal region in the fiber direction (κ_{cf}) is described in eq 1 by that in the chain axis ($\kappa_{c(chain)}$) and the crystal orientation angle ϕ .

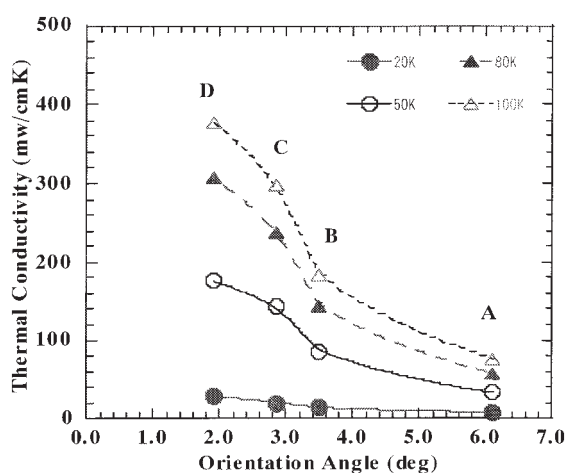


Figure 5. Relation of orientation angles and thermal conductivities at 20, 50, 80, and 100 K of DFs.

Table 1. Parameter of DF(A – D) in the Mechanical Model

| | E (GPa) | Crystallinity (%) | x_{IIc} | x_{IIa} | y_I | y_{II} |
|-------|------------|----------------------|-----------|-----------|-------|----------|
| DF(A) | 15 | 79.5 | 0.782 | 0.218 | 0.058 | 0.942 |
| DF(B) | 51 | 82.7 | 0.781 | 0.219 | 0.213 | 0.787 |
| DF(C) | 85 | 94.7 | 0.918 | 0.082 | 0.354 | 0.646 |
| DF(D) | 134 | 99.0 | 0.978 | 0.022 | 0.544 | 0.455 |

$$\kappa_{cf} = \kappa_{c(\text{chain})} \cos \phi \quad (1)$$

The κ_{cf} of DFs are estimated as follows by eq 1:

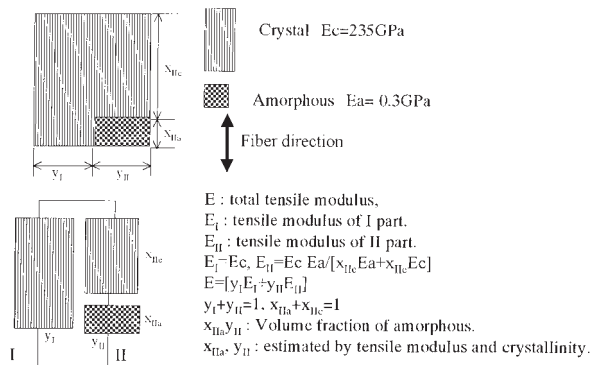
κ_{cf} (A) = 0.994 $\kappa_{c(\text{chain})}$, κ_{cf} (B) = 0.998 $\kappa_{c(\text{chain})}$, κ_{cf} (C) = 0.999 $\kappa_{c(\text{chain})}$, and κ_{cf} (D) = 0.999 $\kappa_{c(\text{chain})}$.

With the aforementioned, the difference of distribution to the thermal conductivity by the crystal orientation angles among the DFs is small in spite of a large difference of thermal conductivities. Therefore, the difference of thermal conductivities among the DFs cannot be explained only by orientation angles. From those results, all DFs are considered as nearly perfect oriented fibers and the chain axes in the crystal regions are considered as fiber axes to discuss thermal conductivity.

In the following section, we use those results to introduce the mechanical series-parallel model to DFs.

Parameters of the Mechanical Series-Parallel Model

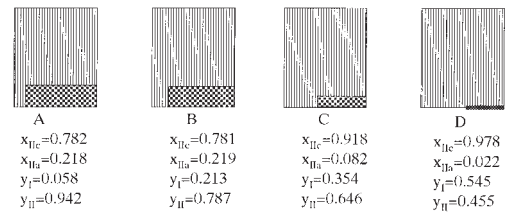
A schematic diagram of the mechanical series-parallel model composed of crystal/amorphous is

**Figure 6.** Schematic diagram showing the structure of DF by mechanical model.

shown in Figure 6. The chain axis in the crystal region is extended and aligned to the fiber axis in this mechanical model, because the orientation angles of DFs are nearly 0 as shown in the earlier sections. As shown in Figure 6, DFs are composed of part I and part II by parallel combination in this model.¹⁷ Part I is continuous crystal, and part II is composed of crystal and amorphous by series combination.¹⁷

The parameters of the mechanical model are defined as follows: E , total tensile modulus in fiber direction; E_I , tensile modulus of part I in fiber axis; E_{II} , tensile modulus of part II in fiber axis; E_c , tensile modulus of crystal in chain axis; E_a , tensile modulus of amorphous; y_I , width of part I; y_{II} , width of part II; x_{IIc} , length of crystal part in part II; x_{IIa} , length of amorphous part in part II; $v_a = x_{IIa} y_{II}$, volume fraction of amorphous. So, crystallinity is shown as $1 - x_{IIa} y_{II}$. Those definitions are also shown in Figure 6. The relation formulas between those parameters are shown in Figure 6. E of DFs are experimental values. E_c is 235GPa obtained by Nakamae and coworkers,⁴¹ and E_a is 0.3GPa obtained by Chen and colleagues.⁴² The volume fractions of amorphous $v_a = x_{IIa} y_{II}$ are estimated by solid state NMR measurements as mentioned above.

The parameters of the mechanical model (x_{IIc} , x_{IIa} , y_I , and y_{II}) were estimated by the substitution of the numerical values aforementioned into the equations shown in Figure 6. The estimated values are shown in Table 1 and Figure 7.¹⁷

**Figure 7.** Schematic diagram of DF(A–D) estimated by the mechanical model.

The Relation Between the Thermal Conductivity and Mechanical Model of DFs

In this section, the mechanical model obtained in the front section is applied to DFs for thermal conductivity. Thermal conductivity of DF in the fiber direction is defined as κ . Thermal conductivity of part I (continuous crystal region) shown in Figure 6 in the chain axis is defined as κ_I , and that of part II shown in Figure 6 in the fiber direction as κ_{II} . κ , κ_I , and κ_{II} are shown in the following eqs 2 and 3:

$$\kappa = y_I \kappa_I + y_{II} \kappa_{II} \quad (2)$$

From $y_I + y_{II} = 1$ as shown in Figure 6,

$$\kappa = (\kappa_I - \kappa_{II})y_I + \kappa_{II} \quad (3)$$

The thermal conductivity of the crystal region in the chain axis is defined as κ_c , and that of the amorphous region as κ_a . Because the orientation angles are nearly 0 as mentioned above, we can neglect contributions by thermal conduction perpendicular to the chain direction. Therefore, the relation between κ_I , κ_{II} , and κ_c , κ_a is shown by eqs 4 and 5 as follows:

$$\kappa_I = \kappa_c \quad (4)$$

$$\kappa_{II} = (\kappa_c \kappa_a) / (\kappa_a X_{IIc} + \kappa_c X_{IIa}) \quad (5)$$

It is known that κ_a is lower than 2 mw/cmK below 150 K.⁸ Meanwhile, thermal conductivity of DF(D) is 500 mw/cmK at 150 K, as shown in Figure 1. Therefore, κ_c is guessed to be higher than 500 mw/cmK, namely, $\kappa_c \gg \kappa_a$. This means that $\kappa_I \gg \kappa_{II}$. From this inequality, eq 3 can be treated as the following eq 6:

$$\kappa \doteq \kappa_I y_I + \kappa_{II} \quad (6)$$

In this mechanical model, eq 6 shows that thermal conductivity (κ) of DF in the fiber direction is dominated by that of part I (κ_I). The value of thermal conductivity in the fiber direction (κ) is expected to depend on that of the crystal region in the chain axis ($\kappa_c (= \kappa_I)$) and the volume fraction of the continuous crystal region (y_I). This approximation was applied to the highly oriented polyethylene for thermal conductivity elsewhere.^{12,14}

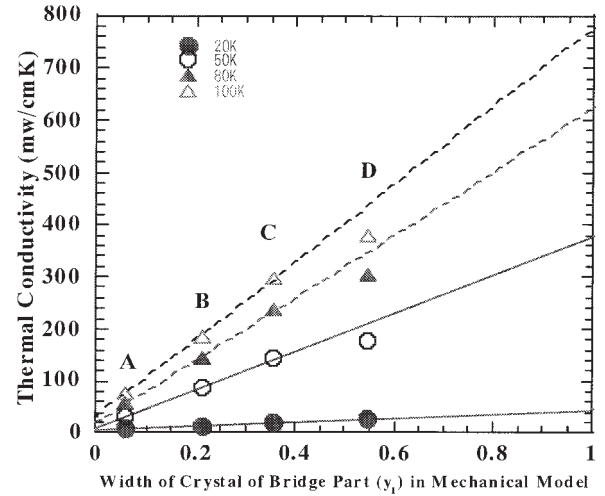


Figure 8. Thermal conductivity of DF(A–D) as functions of y_I in the mechanical model at 20, 50, 80, and 100 K.

We investigate the relation between y_I and thermal conductivity (κ). Thermal conductivity of DF (A–D) as a function of y_I in the mechanical model shown in Table 1 and Figure 7 at 20, 50, 80, and 100 K is shown in Figure 8. Thermal conductivity of DF(A, B, C, D) increases linearly in proportion to y_I . This result shows that eq 3 can be approximated to eq 6. And it also suggests that thermal conductivity of the continuous crystal region ($\kappa_I = \kappa_c$) of every DF is nearly equal. From this section, the mechanical series-parallel model shown in Figure 7 can be applied to DF (A, B, C, D) having different modulus prepared by the same raw material for thermal conductivity.

Thermal Conductivity of Continuous Crystal Region in DFs

In this section, thermal conductivity of the continuous crystal region (part I) (κ_I) is estimated. The parameters of eq 3 can be obtained by linear line approximation of κ and y_I in Figure 8. $\kappa_I = \kappa_c$ can be estimated by extension of the approximated linear line to $y_I = 1.0$, namely, κ_I can be estimated by substitution of $y_I = 1.0$ into eq 3 obtained by linear line approximation. The estimation of κ_I is carried out by every 10 degrees from 10 to 150 K. Temperature dependence of $\kappa_I = \kappa_c$ is shown in Figure 7, with observed thermal conductivity of DFs shown in Figure 1. The κ_c of DF increases from 16 to 900 mw/cmK by the increasing temperature from 10 to 150 K. κ_c increases slowly by increasing temperature.

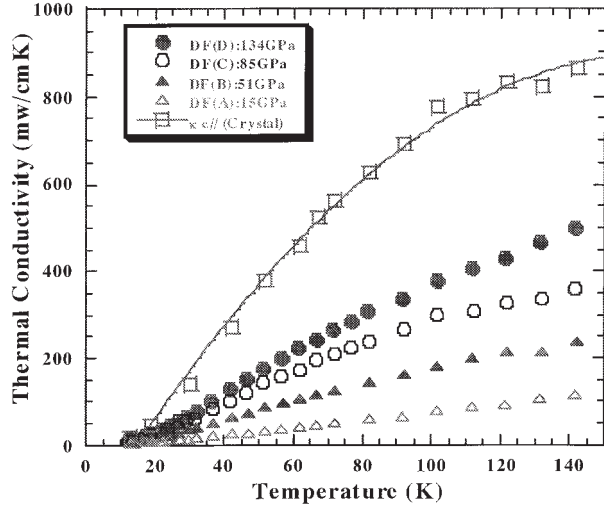


Figure 9. Temperature dependence of thermal conductivity of DF(A–D) and crystal of DF.

Thermal Diffusivity and Phonon Mean Free Path of Continuous Crystal Region in DF

In this section, we estimate thermal diffusivity (λ) of the continuous crystal region in DF. The relation between thermal diffusivity and thermal conductivity is shown in eq 7:

$$\lambda = \kappa / C_p \rho \quad (7)$$

In this equation, C_p is defined as heat capacity and ρ as density of polyethylene. Temperature dependence of the thermal diffusivity λ of the continuous crystal region (part I) is estimated by eq 7. The crystalline density of polyethylene is 1.00 g/cc, which is used as the numerical value of ρ .⁴³ The reported heat capacities⁴³ of polyethylene crystal are used as numerical values of C_p . The C_p is almost orientation independent.⁴³ The values of $\kappa_I = \kappa_c$ shown in Figure 9 are used as κ . λ is estimated by the substitution of the numerical values of κ_c , C_p , and ρ into eq 7. Temperature dependence of thermal diffusivity λ of part I obtained as aforementioned is shown in Figure 10. The obtained λ is about 100 mm²/s at 150 K and nearly temperature independent. The λ increases very slightly with temperature decreasing from 150 K to 40 K, shows minimum value at about 20 K, and increases markedly with temperature decreasing from 20 K to 10 K. In the case of the temperature range under 20 K, both κ and C_p converge to 0 with temperature approaching 0 K. Therefore, the experimental error of $\lambda = \kappa / C_p \rho$ becomes large in this temperature range, so we could not discuss the temperature dependence of λ under 20 K.

From the thermal diffusivity in part I estimated as aforementioned, the mean free path of phonon in the fiber axis of the continuous crystal region in DF is obtained in the following way. The mean free path of phonon l is estimated in eq 8.

$$l = 3\lambda / v \quad (8)$$

In this formula, v is defined as sound velocity. In this case, it is sound velocity in the chain axis in crystal. The v in the chain axis in crystal is estimated by using E_c and ρ in eq 9.

$$v = (E_c / \rho)^{1/2} \quad (9)$$

Tensile modulus of the crystal region in chain direction E_c is assumed as 235 Gpa, reported as the experimental value about DF.⁴¹ And temperature independence of E_c is also reported.⁴¹ On the other hand, estimations of temperature dependence of E_c by calculation are reported.^{44–47} So, more detailed discussion will be necessary for accurate consideration. In this report, the experimental value observed for DF⁴¹ is used as E_c . The density of the crystal region (ρ) is 1.00 g/cc.⁴³ The sound velocity of the crystal in DF (v) is estimated as 15,300 m/s by substitution of the numerical values of E_c and ρ into eq 9. In the case of DF(C), the sound velocity of DF(C) reinforced plastics was measured, and it almost agrees to that estimated tensile modulus.^{48,49}

The mean free path l of phonon of the continuous crystal region of DF in the fiber direction is estimated by the substitution of thermal diffu-

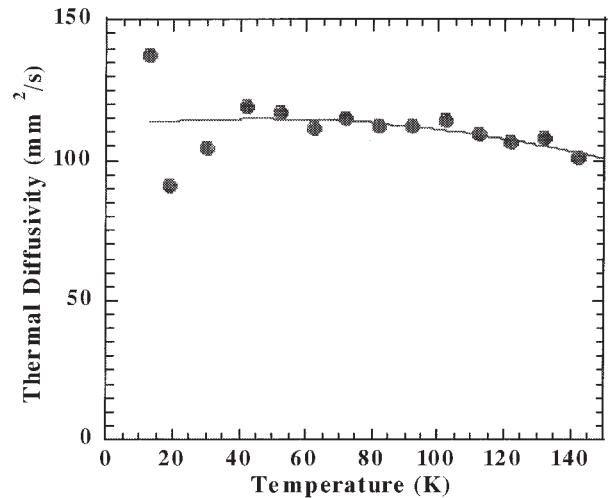


Figure 10. Temperature dependence of thermal diffusivity of the crystal part in DF.

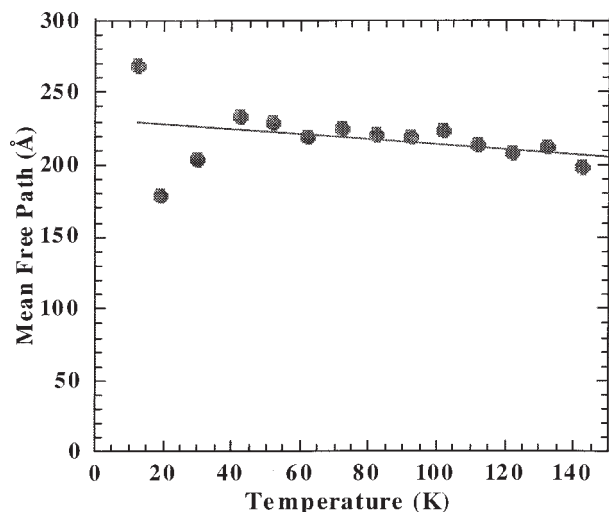


Figure 11. Temperature dependence of the mean free path of phonon in the crystal part in DF.

sivity λ shown in Figure 10 and sound velocity $v = 15,300$ m/s into eq 8. Temperature dependence of the mean free path of phonon (l) in the continuous crystal region is shown in Figure 11. The estimated l is nearly temperature independent and its value about 200 Å. This almost constant l indicates that phonons are mainly scattered by domain wall-like barriers over the entire temperature range. The phonon scattering is inferred to be due to phonon heat conduction in the crystal region. The slight temperature dependence of λ and l shown in Figures 10 and 11 is discussed in the following.

The λ and l were estimated on the following assumptions as aforementioned. The DFs are composed of only two components; crystal and amorphous, and the tensile modulus of the crystal region (E_c) is temperature independent. But more detailed discussion will be necessary to clear the temperature dependence of E_c as aforementioned. The change of E_c reported by other articles^{44–47} is 4 ~ 60GPa by cooling from 300 K to 4 K. This increasing of E_c means a slight increasing of sound velocity and λ .

On the other hand, it is reported that polyethylene has many components, for example, intermediate regions between crystal and amorphous.^{38–40} In the case of DF, it was reported that the crystalline signal of DF in NMR is composed of several components.^{39,40} Therefore, the crystal region in the mechanical model in this article is able to contain the components' amorphous-like crystal or crystal-like amorphous to add to the crystal region. The tensile modulus of those components is able to increase with

decreasing temperature. This means that the sound velocity and λ increase with temperature decrease. The detailed discussion about the morphology and temperature dependence of E_c of DF will be necessary to clear the slight temperature dependence of λ and l .

CONCLUSIONS

Thermal conductivity, crystallinity, and orientation angles were measured for several kinds of high strength polyethylene fiber (DF (A–D)) having different modulus, which were 15–134GPa. And a mechanical series parallel model composed of extended crystal and amorphous (the Takayanagi model) was applied to DFs for thermal conductivity. The following conclusions were drawn:

1. Thermal conductivity increases with increasing tensile modulus of DF.
2. In this mechanical model composed of a continuous crystal region and a series combination part composed of crystal and amorphous, thermal conductivity (κ) of DF in the fiber direction is dominated by that of the continuous crystal region.
3. The thermal conductivity of the continuous crystal region in DF increases from 16 to 900 mw/cmK by increasing temperature from 10 to 150 K.
4. The thermal diffusivity of the continuous crystal region in DF is about 100 mm²/s and is almost temperature independent.
5. The phonon mean free path of the continuous crystal region of DF obtained by thermal diffusivity is almost temperature independent and its value about 200 Å.

With the aforementioned, the mechanical series-parallel model composed of crystal and amorphous could be applied to DFs for thermal conductivity.

The authors thank Dr. Yasuo Ohta and Dr. Tadao Kuroki of Toyobo Co., Ltd. for preparing DF samples. The authors also thank professor Dr. Masakatsu Takeo of Kyushu University, professor Dr. Tomoaki Takao of Sophia University, and professor Dr. Kenji Hosoyama of the High Energy Accelerator Research Organization for useful suggestions about the importance of thermal conductivity of materials for applied superconductivity. Thanks to professor Dr. Yuichi Okuda and Dr. Ryuji Nomura of the Tokyo Institute of Technology for useful suggestion about the sound velocity of DF. Thanks also to the experimental assistant group of the Polymer

Institute in Toyobo Research Center Co., Ltd. for experimental assistance. Thanks to Dr. Hiroshi Hirahata, Dr. Yukihiko Nomura, and members in the advanced textiles R and D center of Toyobo, Co, Ltd. for useful discussions. Thanks to the Dyneema Department of Toyobo, Co, Ltd. for encouragement.

REFERENCES AND NOTES

- Bhowmick, T.; Pattanayak, S. *Cryogenics* 1990, 30, 116.
- Jackel, M.; Muller, M.; Claverie, A. L.; Arndt, K. F. *Cryogenics* 1991, 31, 228.
- Choy, C. L.; Wong, S. P.; Young, K. *J Polym Sci, Polym Phys Ed* 1985, 23, 1495.
- Choy, C. L.; Leung, W. P. *J Polym Sci Polym Phys Ed* 1983, 21, 1243.
- Mergenthaler, D. B.; Pietralla, M.; Roy, S.; Killian, H. G. *Macromolecules* 1992, 25, 3500.
- Burgess, S.; Greig, D. *J Phys C: Solid State Phys* 1975, 8, 1637.
- Gibson, A. G.; Greig, D.; Sahota, M.; Ward, I. M.; Choy, C. L. *J Polym Sci Polym Lett Ed* 1977, 15, 183.
- Choy, C. L. *Polymer* 1977, 18, 984.
- Choy, C. L.; Luk, W. H.; Chen, F. C. *Polymer* 1978, 19, 155.
- Fujishiro, H.; Ikebe, M.; Kashima, T.; Yamanaka, A. *Jpn J Appl Phys* 1997, 36, 5633.
- Fujishiro, H.; Ikebe, M.; Kashima, T.; Yamanaka, A. *Jpn J Appl Phys* 1998, 37, 1994.
- Gibson, A. G.; Greig, D.; Ward, I. M. *J Polym Sci Polym Phys Ed* 1980, 18, 1481.
- Mugishima, T.; Kogure, Y.; Hiki, Y.; Kawasaki, K.; Nakamura, H. *J Phys Soc Jpn* 1988, 57, 2069.
- Choy, C. L.; Chen, F. C.; Luk, W. H. *J Polym Sci Polym Phys Ed* 1980, 18, 1187.
- Scholle, K. F. M. J. 9th Int SAMPE, European Chapter, Milano, Italy, June 14–16, 1988.
- Kashima, T.; Yamanaka, A.; Takasugi, S.; Nishihara, S. *Adv Cryog Eng* 2000, 46, 329.
- Yamanaka, A.; Kitagawa, T.; Tsutsumi, M.; Kashima, T.; Fujishiro, H.; Ema, K.; Izumi, Y.; Nishijima, S. *J Appl Polym Sci* 2004, 93, 2918.
- Kashima, T.; Yamanaka, A.; Nishijima, S.; Okada, T. *Adv Cryog Eng* 1996, 42, 147.
- Kamijo, H.; Nemoto, K.; Kashima, T. *Proc. of Meeting on Cryogenics and Superconductivity* 1993, 105.
- Kashima, T.; Yamanaka, A.; Yoneda, E. S.; Nishijima, S.; Okada, T. *Adv Cryog Eng* 1996, 41, 441.
- Yamanaka, A.; Kashima, T.; Nishijima, S.; Okada, T. *Cryog Eng* 1998, 33, 710.
- Takao, T.; Watanabe, K.; Kubosaka, T.; Suzuki, T.; Kashima, T.; Yamanaka, A.; Fukui, S. *IEEE Trans Appl Supercond* 1999, 9, 1133.
- Takeda, K.; Chiba, M.; Fukuda, K.; Sakagami, Y.; Shibuya, M.; Miyashita, K.; Moriai, H.; Kamata, K. *Proc of ICEC* 1999, 17.
- Yamanaka, A.; Kashima, T.; Nishijima, S.; Okada, T. *Cryog Eng* 2000, 35, 530.
- Yamanaka, A.; Kashima, T.; Hosoyama, K. *IEEE Trans Appl Supercond* 2001, 11, 4061.
- Yamanaka, A.; Kashima, T.; Nishijima, S.; Takao, T.; Takeo, M. *Cryog Eng* 2001, 36, 525.
- Yamanaka, A.; Kashima, T.; Hosoyama, K.; Nago, S.; Takao, T.; Sato, S.; Takeo, M. *Phys C: Supercond* 2002, 372–376, 1447.
- Takeo, M.; Sato, S.; Matsuo, M.; Kiss, T.; Takao, T.; Yamanaka, A.; Kashima, T.; Mito, T.; Minamizato, K. *Cryogenics* 2003, 43, 649.
- Hoshino, T.; Salim, K. M.; Muta, I.; Nakamura, T.; Yamada, M.; Yamanaka, A. *Proc. of Meeting on Cryogenics and Superconductivity* 2004, 70, 22.
- Yamanaka, A.; Kashima, T.; Nishijima, S.; Okada, T. *Cryog Eng* 1997, 32, 330.
- Mito, T.; Kawagoe, A.; Chikaraishi, H.; Okumura, K.; Seo, K.; Maekawa, R.; Henmi, T.; Abe, R.; Baba, T.; Yokota, M.; Morita, Y.; Yamauchi, K.; Hayashi, K.; Iwakuma, M.; Sumiyoshi, F. *Proc. of Meeting on Cryogenics and Superconductivity* 2004, 70, 101.
- Takao, T.; Kawasaki, A.; Yamaguchi, M.; Yamamoto, H.; Niino, A.; Nakamura, K.; Yamanaka, A. *Proc of ASC* 2002, 2002.
- Takao, T.; Yamaguchi, M.; Yamamoto, H.; Yamanaka, A. *Proc of EUCAS* 2003, 2003.
- Nitta, T.; Chiba, M.; Kasima, T.; Takao, T. *Proc of 15th Int Conf MT* 1997, 1159.
- Fujishiro, H.; Ikebe, M.; Naito, T.; Noto, K. *Cryog Eng* 1993, 28, 533.
- Vanderhart, D. L.; Khoury, F. *Polymer* 1984, 25, 2589.
- Yamanobe, T.; Sorita, T.; Komoto, T.; Ando, I.; Sato, H. *J Mol Struct* 1985, 131, 267.
- Kitamaru, R.; Horii, F.; Murayama, M. *Macromolecules* 1986, 19, 636.
- Kaji, A.; Ohta, Y.; Yasuda, H.; Murano, M. *Polym J* 1990, 22, 455.
- Kaji, A.; Yamanaka, A.; Murano, M. *Polym J* 1990, 22, 893.
- Nakamae, K.; Nishino, T.; Ohkubo, H. *J Macromol Sci Phys* 1991, 30, 1.
- Chen, C. F.; Choy, C. L.; Young, K.; Wong, S. *J Polym Sci Polym Ed* 1981, 19, 971.
- Gaur, U.; Wunderlich, B. *J Phys Chem Ref Data* 1981, 10, 119.
- Shimanouchi, T.; Asahina, M.; Enomoto, S. *J Polym Sci* 1962, 59, 93.
- Tashiro, K.; Kobayashi, M.; Tadokoro, H. *Macromolecules* 1977, 10, 731.
- Karasawa, N.; Dasgupta, S.; Goddard, III, W. A., *J Phys Chem* 1991, 95, 2260.
- Tashiro, K. *Polymer Preprint* 1999, 3867.
- Nomura, R.; Yoneyama, K.; Ogasawara, F.; Ueno, M.; Okuda, Y.; Yamanaka, A. *Jpn J Appl Phys* 2003, 42, 5205.
- Nomura, R.; Ueno, M.; Okuda, Y.; Burmistrov, S.; Yamanaka, A. *Physica B: Condens Matter* 2003, 329–333, 1664.